

CrystEngComm

Accepted Manuscript



This is an *Accepted Manuscript*, which has been through the Royal Society of Chemistry peer review process and has been accepted for publication.

Accepted Manuscripts are published online shortly after acceptance, before technical editing, formatting and proof reading. Using this free service, authors can make their results available to the community, in citable form, before we publish the edited article. We will replace this *Accepted Manuscript* with the edited and formatted *Advance Article* as soon as it is available.

You can find more information about *Accepted Manuscripts* in the [Information for Authors](#).

Please note that technical editing may introduce minor changes to the text and/or graphics, which may alter content. The journal's standard [Terms & Conditions](#) and the [Ethical guidelines](#) still apply. In no event shall the Royal Society of Chemistry be held responsible for any errors or omissions in this *Accepted Manuscript* or any consequences arising from the use of any information it contains.

Cite this: DOI: 10.1039/c0xx00000x

www.rsc.org/crystengcomm

PAPER

Water/*n*-heptane interface as a viable platform for self-assembly of ZnO nanospheres to nanorods

Mohammed Ali, Hasimur Rahaman, Dewan S. Rahman, Surjatapa Nath and Sujit Kumar Ghosh*

Received (in XXX, XXX) Xth XXXXXXXXXX 20XX, Accepted Xth XXXXXXXXXX 20XX

DOI: 10.1039/b000000x

Water/*n*-heptane interface has been exploited as a viable and selective platform for the transformation of quasi-spherical ZnO nanoparticles to nanorods using non-conventional low precursor salt concentration under facile and benign reaction condition. The transformation of nanospheres to nanorods has been characterised by absorption, fluorescence, Fourier transform infrared spectroscopy, X-ray diffraction pattern and transmission electron microscopy. The mechanism of transformation to nanorods from the ultrasmall ZnO particles in the restricted environment provided by liquid-liquid interface has been elucidated.

1. Introduction

In recent years, the self-assembly of nanoscale objects paves a simple and general strategy to organise nanoparticles into higher order architectures.¹ Such processes require adequate stabilisation of the nanoparticles at interfaces with a high degree of organisational selectivity.^{1,2} Amongst the three different approaches that are currently exploited to effect ordering of nanoparticles by the self-assembly processes, liquid-liquid interfaces offer an important alternative scaffold for the colloidal crystallisation into higher ordered nanostructures.² A number of innovative approaches have been explored to engender interfacial ordering effects for the organisation of nanometer-size objects into both two and three dimensions, including, membranes,³ capsules,⁴ core-shell structures,⁵ heterodimeric alloyed nanostructures,⁶ Janus particles,⁷ and giant supramolecular assemblies⁸ with distinct functionalities. Semiconductor zinc oxide (ZnO) nanoobjects have attracted immense interests due to its direct wide band gap (3.37 eV), high exciton binding energy (60 meV) and the opportunity to vary its properties by morphological tunability.⁹ One-dimensional semiconductor (ZnO) nanostructures (nanowires and nanorods) have attracted special interest due to their fascinating physical properties and potential applications in electronic and photonic devices.⁹

Varieties of synthetic strategies have been adopted in the literature for the fabrication of ZnO nanorods, for example, high temperature physical evaporation,¹⁰ micro-emulsion based hydrothermal process,¹¹ alcohol thermal process¹² and so on. Yin et al.¹³ have reported the synthesis of ZnO quantum nanorods by thermal decomposition of zinc acetate (40 mM) in organic

solvents in the presence of oleic acid 286 °C for 1 h under N₂ flow. Wang and colleague¹⁴ have designed the directed growth of ZnO nanorod arrays on zinc substrate by alkaline hydrolysis of zinc foils (15×15×0.25 mm³) in the presence of cetyltrimethylammonium bromide loaded into a Teflon-lined stainless steel autoclave by heating at 160 °C for 20 h. Ho and co-authors¹⁵ have developed a solution-based synthesis to grow highly ordered ZnO nanorods-like structures on selective areas of the substrate by heating zinc acetate (5-10 mM) at 90 °C for 8 h in a tight polypropylene screw cap. Guo et al.¹⁶ reported the synthesis of ZnO nanorods by ripening the mixture of zinc acetate (50 mM) and potassium hydroxide in methanol at 70 °C, at least, for three days to achieve a narrow size distribution. Weller group¹⁷ have investigated that, in a methanolic solution, at a zinc acetate dihydrate concentration of below 10 mM, quasi-spherical particles are formed; whereas, mainly nanorods are formed at ten times higher concentration of the precursor. In general, these synthetic methods are carried out at high concentration of the precursor salt by forced hydrolysis in the presence or absence of a weak base. In this communication, we have investigated that water/*n*-heptane interface could offer a viable platform for the self-assembly of ZnO nanodots to nanorods using non-conventional low precursor salt concentration (1.0 mM) under facile and benign reaction condition.

2. Experimental section

2.1. Reagents and instruments

All the reagents used were of analytical reagent grade. Zinc(II) acetate dihydrate, [Zn(OOCCH₃)₂ · 2H₂O] and potassium hydroxide (KOH), were purchased from Sigma Aldrich and used as received. All the solvents *viz.*, *n*-heptane, benzene, toluene, dichloromethane, cyclohexane and *o*-xylene were purchased from Sisco Research Laboratories and used without further purification. Double distilled water was used throughout the

Department of Chemistry, Assam University, Silchar-788011, India

Fax: +91-3842-270802; Tel: +91-3842-270848;

E-mail: sujit.kumar.ghosh@aus.ac.in

course of the investigation. The temperature was 298 ± 1 K during the experiments.

Absorption spectra were recorded on Shimadzu UV 1601 digital spectrophotometer (Shimadzu, Japan) taking the sample in 1 cm quartz cuvette. Fluorescence spectra were recorded with a Perkin Elmer LS-45 spectrofluorometer (Perkin Elmer, UK). Fourier transform infrared (FTIR) spectra were recorded in the form of pressed KBr pallets in the range ($400\text{--}4000\text{ cm}^{-1}$) in Shimadzu-FTIR Prestige-21 spectrophotometer. Transmission electron microscopic (TEM) measurements were performed on carbon-coated copper grids with a Zeiss CEM 902 operated at 80 kV. Powder X-ray diffraction patterns (XRD) were obtained using a D8 ADVANCE BROKERaxs X-ray Diffractometer with $\text{CuK}\alpha$ radiation ($\lambda = 1.4506\text{ \AA}$); data were collected at a scan rate of $0.5^\circ\text{ min}^{-1}$ in the range of $10^\circ\text{--}80^\circ$.

2.2. Synthesis of ZnO nanomaterials

In a typical experiment, an amount of 0.055 g zinc acetate dihydrate was dissolved in 25 mL of solvent mixture (water : *n*-heptane = 9 : 1) in a double-naked round-bottom flask by refluxing on a water bath at 65°C . After 15 min, 13.5 mL aqueous KOH solution (0.1 mM) was added to the mixture and the refluxing was continued for another 2 h. It was seen that, initially, a faint yellow colouration so appeared slowly transformed to curdy white indicating progressive transformation of nuclei into larger particles.¹¹ Finally, the mixture was cooled to room temperature and stored in the dark.

3. Results and discussion

The progressive transformation of the ultrasmall ZnO particles into larger aggregates has been studied by UV-vis absorption, fluorescence, Fourier transform infrared (FTIR), X-ray diffraction (XRD) spectroscopy and transmission electron microscopy (TEM). Fig. 1 represents the absorption spectra showing the time evolution of the primarily formed ZnO particles into larger aggregates and the fluorescence spectrum of the finally formed particles synthesised at water/*n*-heptane interface at different time intervals. At the beginning, the absorption spectrum shows two maxima, one at 219 nm (5.66 eV) and the other at 265 nm (4.68 eV), which are the characteristics of spherical ZnO nanoparticles. In case of semiconductor nanoparticles, the Fermi energy level lies in-between the valance and conduction band, which

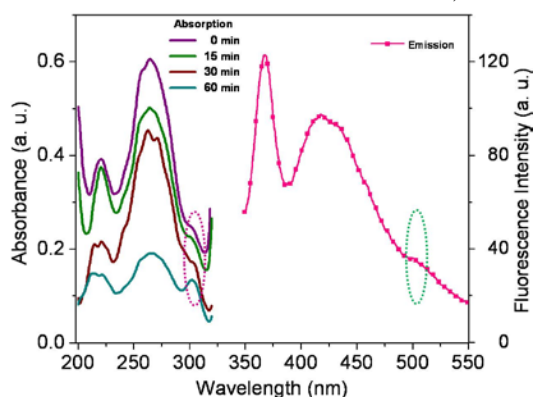


Fig.1. Absorbance and fluorescence spectra showing the evolution of ZnO nanospheres to nanorods

comprises of discrete energy states due to strong electron confinement. These two peaks arise due to the excitonic transitions between the trapped energy states situated in between the confinement region.¹⁸ Size of the intervening gaps are correlated with the band structure, which again depends on the size of the nanoparticles on basis of the interaction with the confined electrons among the lattice points. The optical band edge bears the characteristic electronic transition energy taken place to promote the electrons to the energy states in conduction band from the valence band, including excitonic effects. As the time progresses, both the peaks decrease in intensity and a new peak at 302 nm (4.11 eV) develops indicating the gradual transformation of ZnO nanospheres to nanorods.¹⁶ The fluorescence spectrum ($\lambda_{\text{ex}} \sim 302\text{ nm}$) of the finally formed ZnO particles exhibit a narrow emission band at 379 nm (3.27 eV) that is attributed to the radiative recombination of a hole in the valence band and an electron in the conduction band (excitonic emission).¹⁶ In addition, trace of two emission peaks at *ca.* 416 nm (2.98 eV) and 434 nm (2.86 eV) are seen that could be attributed to the presence of multiple surface defects in the ZnO nanorods.¹⁹ The absorption and fluorescence spectra, thus, indicates the progressive transformation of the ZnO nanospheres to nanorods.

Fig. 2 shows the corresponding TEM images of the ZnO particles at the beginning and end of the reaction. It is seen that the initial particles are quasi-spherical in nature with average

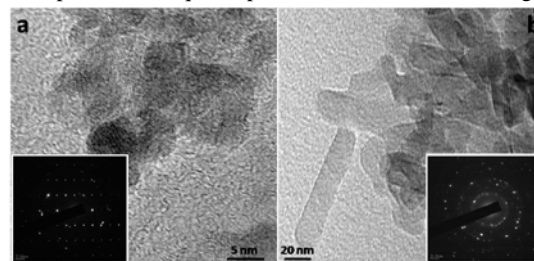


Fig. 2. Representative TEM images of ZnO particles at the (a) beginning and (b) end of the reaction. Insets show the corresponding selected area electron diffraction pattern of the ZnO nanostructures.

particle sizes 3-5 nm while the rod-shaped particles are *ca.* 100 – 200 nm and 15-20 nm in length and diameter, respectively. The corresponding selected area electron diffraction patterns (shown in the inset) reveal the appearance of polycrystalline-like diffraction which are consistent with reflections (100), (002), (101), (102), (110) corresponding to the hexagonal wurtzite phase of ZnO particles indicating that the nanorod is an ordered assembly of small nanocrystal sub-units without crystallographic orientation.²⁰

Detailed TEM investigations during the formation of the nanorods are presented in Fig. 3. At low magnification, aggregated quasi-spherical particles are seen (panel a) and subsequently, form pearl-chain-like structures (panel b). It could be recognised that the particles are epitaxially fused together and bottlenecks between the adjacent attachment is seen along the *c*-axis (002), but lateral oriented attachment parallel to the *c*-axis is also evident (panel c). In some cases, it is apparent that the individual particles are aligned like a wall, where the second layer of bricks is just started to be put on the particles are still

visible. Therefore, it is evident that the nanorods are formed by coalescence through ‘oriented attachment’ of quasi-spherical particles. This model of transformation of ZnO nanospheres to nanorods has been evidenced by Weller group.¹⁷ Oriented attachment has, previously, been proposed by other authors during crystal growth of iron oxide, TiO₂ with sizes of a few nm and for micrometer sized ZnO particles during the formation of rod-like ZnO microcrystals.²¹⁻²³

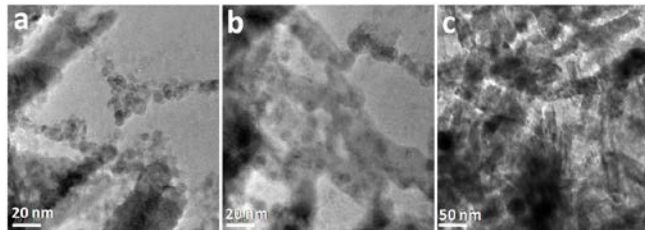


Fig. 3. TEM investigations during the transformation of nanorods (a) 15, (b) 30 and (c) 45 min of reflux.

Fig. 4 shows the high resolution TEM images of single ZnO nanorods with various magnifications. It is seen that the lattice planes of the depicted nanorods are almost perfectly aligned with a lattice fringe of 0.26 nm consistent with the d_{002} spacing of wurtzite ZnO nanostructures.²⁴ Moreover, it could be recognised that the lattice planes go straight through the contact areas of the small spherical nanocrystals.

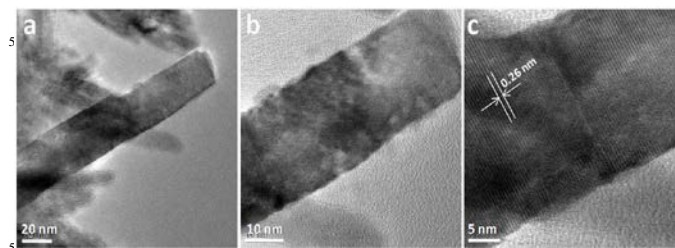


Fig.4. TEM images of ZnO nanorods with increasing magnifications

Fig. 5 is the FTIR spectra of as-growing ZnO nanostructures at different time intervals. With increasing reflux time, it is seen that a peak at *ca.* 458 cm⁻¹, assigned to stretching vibration of Zn–O bonds, is sharpening with time indicating the crystallization of ZnO into higher order architectures.²³ Moreover, other peaks at *ca.* 805, 853 and 863 cm⁻¹ exhibit similar trends with increasing reflux time.²⁵ In addition, strong absorption at 3,442 cm⁻¹ and weak absorptions around 2,800 to 3,000 cm⁻¹ region reveal the stretching vibrations of O–H and C–H, respectively. The absorption peak at 1,104 cm⁻¹ corresponds to the C–OH stretching and O–H bending vibrations, whereas the bands at 1,383, 1,577, and 1,630 cm⁻¹ correspond to C–O (hydroxyl, ester, or ether) stretching and O–H bending vibrations.²⁶ Therefore, it could be conceived that the dominant growth mechanism of ZnO nanorods is mainly the oriented attachment mechanism. The concomitant appearance of other bands indicates the presence of organic residues on the surface of nanospheres and even after the formation of nanorods.

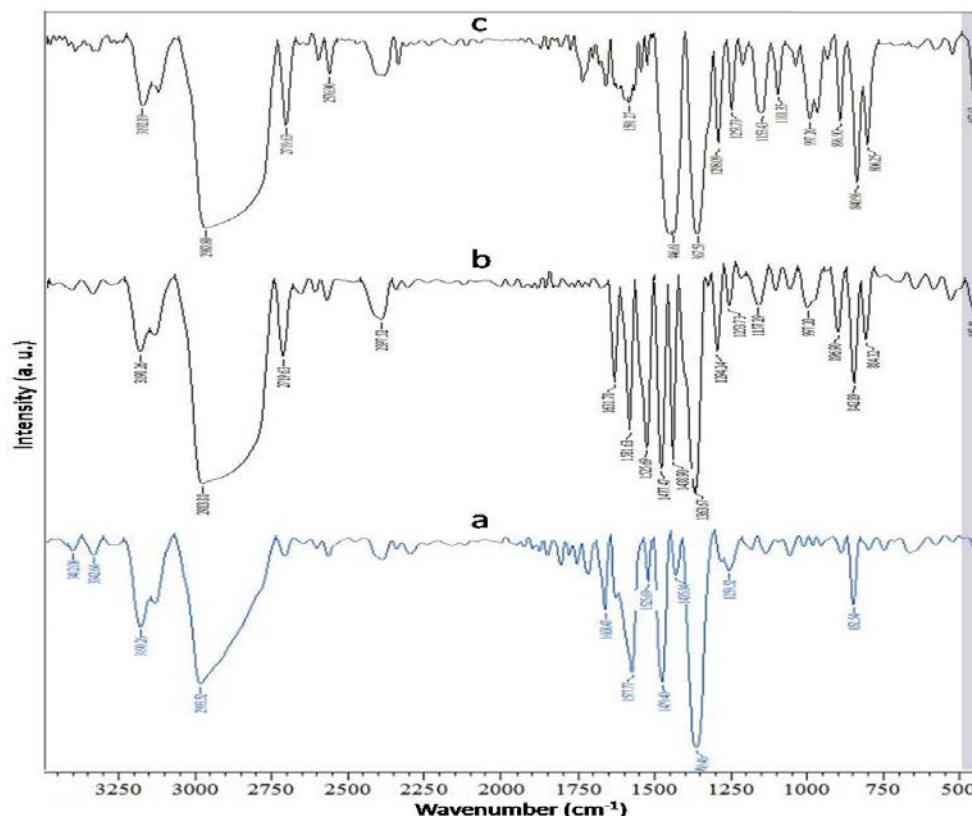


Fig. 5. FTIR spectra during the transformation of ZnO nanospheres to nanorods after (a) 0, (b) 30 and (c) 90 min of reflux. The shaded area indicates the area of interest.

X-ray diffractograms of as-prepared ZnO samples with various reflux times are shown in Fig. 6. All patterns could be indexed to pure hexagonal phase of Zn with a space group of C_{6v}^4 and cell constants $a = 3.25 \text{ \AA}$, and $c = 5.21 \text{ \AA}$ (JCPDS card No.: 76-0704), which suggests that the product comprises ZnO nanocrystals with the wurtzite structure.²⁷ An increase in refluxing time, increases the relative intensities of the (002) diffraction line which is consistent with the rod formation along the c-axis of the particles.²⁴

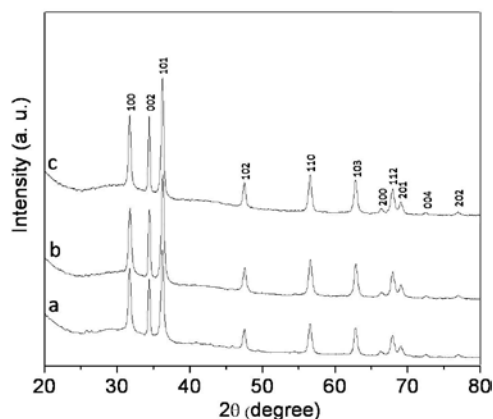
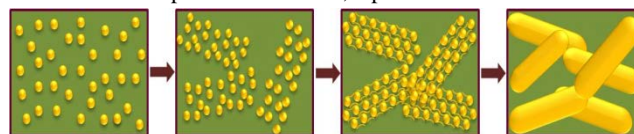


Fig. 6. X-ray diffractograms of the transformation of ZnO nanospheres to nanorods (a) 30 min, (b) 1 h and (c) 2 h of reflux.

To elucidate the mechanism of transformation of ZnO nanospheres to nanorods at the liquid-liquid interface, a series of experiments were carried out. It is noted that the transformation to nanorods does not occur at the prescribed low precursor concentration in the presence of polar solvents in consistent with earlier observation.¹⁷ The formation of the nanorods was tried in the presence of six water-immiscible solvents *viz.*, cyclohexane, *n*-heptane, benzene, toluene, *o*-xylene and dichloromethane and the fluorescence spectra ($\lambda_{\text{ex}} \sim 302 \text{ nm}$) of the finally formed particles were measured (ESI 1). It is seen that the appearance of a new band at 503 nm only in the presence of *n*-heptane led us curious about the uniqueness of the morphology of the particles formed at the water/*n*-heptane interface. The TEM images of the particles formed in the presence of two other representative solvents *viz.*, dichloromethane and cyclohexane are shown (ESI 2). The transformation of the quasi-spherical particles to rods was not seen in any of these solvents. It is, now, well-established in the literature that the formation of the nanorods requires anisotropic crystal growth based on the surface and attachment energies of various crystallographic planes.^{17,21-23} While the present experiment is carried out in the absence of organic solvent keeping all other experimental conditions unaltered, there is the formation of ultrasmall ZnO nanoparticles. Therefore, it could be conceived that water/*n*-heptane interfacial tension offers the requisite restricted environment for the oriented attachment of the nanospheres to nanorods. The composition of the solvent also plays a role for the transformation of nanospheres to nanorods. The fluorescence spectra obtained by varying water/*n*-heptane composition is shown in ESI 3. It is seen that the appearance of a new band at 503 nm only in the presence of *n*-heptane at a

volume ratio of water : *n*-heptane = 9 : 1; at a volume ratio above or below, the appearance of no such band is observed. Therefore, it could be concluded that formation of the nanorods is favoured at an optimum composition of the water and *n*-heptane mixture. It is, now, well established in the literature that a liquid-liquid interface is a non-homogeneous region having a thickness of the order of a few nanometers.²⁸ The interface between two immiscible liquids, thus, offers an important scaffold for the chemical manipulation and self-assembly of the nanocrystals.²⁹ The interfacial tension at the water/*n*-heptane interface is dependent upon solvent composition. Therefore, it is manifested that while the liquid-liquid interface offers a viable platform, the observed assembly is the result of specific interparticle interactions harnessing the transformation to nanorods. The attachment does not occur at room temperature pointing out that a moderately higher temperature (65 °C; below the boiling point of *n*-heptane, 98.42 °C) helps to tailor the fusion of the particles. When two ZnO building blocks come together, the capillary forces between them facilitates the solvent removal and strengthen the agglomerate by van der Waals' forces. Finally, with increase in reaction time, directed self-assemblies of the oriented nanocrystallites and subsequent fusion lead to the formation of ZnO one-dimensional nanorods.³⁰ Therefore, on the basis of above experimental results, a plausible mechanism for



Scheme 1. Schematic presentation of the formation of nanorods from nanospheres

the transformation of ZnO nanospheres to nanorods through the oriented attachment of the ultrasmall particles could be enunciated as depicted in Scheme 1.

4. Conclusions

Liquid-liquid interface has been exploited as a viable platform for the oriented attachment of quasi-spherical ZnO nanoparticles to single crystalline nanorods under the prescribed reaction conditions. The formation of ZnO nanorods could be achieved at very low concentration of the precursor in a restricted environment created by a particular composition of polar/non-polar liquid pairs. Incidentally, the transformation occurs selectively at the water/*n*-heptane interface offering the nanorods under environmentally benign conditions.

Acknowledgements

We gratefully acknowledge financial support from DST, New Delhi (Project No.: SR/FT/CS-68/2010).

Supporting Information. Fluorescence spectra and TEM images. This material is available free of charge at <http://www.rsc.org>.

Notes and references

1. E. Katz, A. N. Shipway, I. Willner, In *Nanoscale Materials* (Eds.: L. M. Liz-Marzan, V. P. Kamat), Kluwer, Norwell, 2003, pp. 317–343.
2. W. H. Binder, *Angew. Chem. Int. Ed.* 2005, **44**, 5172–5175.
3. Y. Lin, H. Skaff, A. Böker, A. D. Dinsmore, T. Emrick, T. P. Russell, *J. Am. Chem. Soc.* 2003, **125**, 12690–12691.
4. H. Duan, D. Wang, D. G. Kurth, H. Möhwald, *Angew. Chem. Int. Ed.* 2004, **43**, 5639–5642.
5. Z. Niu, J. He, T. P. Russel, Q. Wang, *Angew. Chem. Int. Ed.* 2010, **49**, 10052–10066.
6. H. Gu, Z. Yang, J. Gao, C. K. Chang, B. Xu, *J. Am. Chem. Soc.* 2005, **127**, 34–35.
7. A. H. Gröschel, A. Walther, T. I. Löbbling, J. Schmelz, A. Hanisch, H. Schmalz, A. H. E. Müller, *J. Am. Chem. Soc.* 2012, **134**, 13850–13860.
8. M. Ali, S. K. Pal, H. Rahaman, S. K. Ghosh, *Soft Matter*, 2014, **10**, 2767–2774.
9. Z. L. Wang, *Appl. Phys. A* 2007, **88**, 7–15.
10. Y. W. Wang, L. D. Zhang, D. J. Wang, X. S. Peng, Z. Q. Chu, C. H. Liang, *J. Cryst. Growth*, 2002, **234**, 171–175.
11. J. Zhang, L. D. Sun, H. Y. Pan, C. S. Liao, C. H. Yan, *New J. Chem.* 2002, **26**, 33–34.
12. J. B. Cheng, X. B. Zhang, X. Y. Tao, H. M. Lu, Z. Q. Luo, F. Liu, *J. Phys. Chem. B* 2006, **110**, 10348–10353.
13. M. Yin, Y. Gu, I. L. Kuskovsky, T. Andelman, Y. Zhu, G. F. Neumark, S. O'Brien, *J. Am. Chem. Soc.* 2004, **126**, 6206–6207.
14. D. Wang, C. Song, *J. Phys. Chem. B* 2005, **109**, 12697–12700.
15. C. H. Wang, A. S. W. Wong, G. W. Ho *Langmuir* 2007, **23**, 11960–11963.
16. Y. Guo, X. Cao, X. Lan, C. Zhao, X. Xue, Y. Song, *J. Phys. Chem. C* 2008, **112**, 8832–8838.
17. C. Pacholski, A. Kornowski, H. Weller, *Angew. Chem. Int. Ed.* 2002, **41**, 1188–1191.
18. A. P. Alivisatos, *Science* 1996, **271**, 933–937.
19. M. L. Kahn, T. Cardinal, B. Bousquet, M. Monge, V. Jubera, B. Chaudret, *Chem. Phys. Chem.* 2006, **7**, 2392 – 2397.
20. M. Y. Ge, H. P. Wu, L. Niu, J. F. Liu, S. Y. Chen, P. Y. Shen, Y. W. Zeng, Y. W. Wang, G. Q. Zhang, J. Z. Jiang, *J. Cryst. Growth* 2007, **305**, 162–166.
21. J. F. Banfield, S. A. Welch, H. Zhang, T. T. Ebert, R. L. Penn, *Science* 2000, **289**, 751–754.
22. A. Chemseddine, T. Moritz, *Eur. J. Inorg. Chem.* 1999, 235–245.
23. M. Andres Verges, A. Mifsud, C. J. Serena, *J. Chem. Soc. Faraday Trans.* 1990, **86**, 959–963.
24. D. Krishnan, T. Pradeep, *J. Cryst. Growth* 2009, **311**, 3889–3897.
25. K. M. Joshi, V. S. Shrivastava, *Appl. Nanosci.* 2011, **1**, 147–155.
26. M. Sevilla, A. B. Fuertes, *Chem. Eur. J.* 2009, **15**, 4195–4203.
27. M. Goano, F. Bertazzi, M. Penna, E. Bellotti, *J. Appl. Phys.* 2007, **102**, 083709–083719.
28. A. Böker, J. He, T. Emrick, T. P. Russell, *Soft Matter* 2007, **3**, 1231–1248.
29. D. Nykypanchuk, M. M. Maye, D. van der Lelie, O. Gang, *Nature* 2008, **451**, 549–552.
30. M. Fernández-García, J. A. Rodríguez, In *Nanomaterials: Inorganic and Bioinorganic Perspectives*, (Eds: C. M. Lukehart, R. A. Scott) John Wiley & Sons, West Sussex, UK 2008, p. 453.

Table of Contents (TOC)

Water/*n*-heptane interface as a viable platform for self-assembly of ZnO nanospheres to nanorods

Mohammed Ali, Hasimur Rahaman, Dewan S. Rahman, Surjatapa Nath and Sujit Kumar Ghosh

Water/*n*-heptane interface has been exploited as a **viable and selective platform** for the **transformation of quasi-spherical ZnO nanoparticles to nanorods**.

